

# Molecular Modeling of Polymer Flammability: Application to the Design of Flame-Resistant Polyethylene

Marc R. Nyden,\* Glenn P. Forney, and James E. Brown

Building and Fire Research Laboratory, National Institute of Standards and Technology, Gaithersburg, Maryland 20899

Received October 4, 1991; Revised Manuscript Received November 26, 1991

**ABSTRACT:** Molecular dynamic simulations of the thermal degradation of polyethylene were used to identify factors which might be effective in reducing polymer flammability by promoting the formation of a residual char. Computer movies of the calculated trajectories indicate that cross-linked polymers, such as those obtained from exposure of polyethylene to ionizing radiation, will undergo further cross-linking when burned, eventually forming a high molecular weight, thermally stable char. This prediction was confirmed in flammability tests of  $\gamma$ -ray-irradiated polyethylene.

## Introduction

The demand for better, cheaper, and safer materials has led to a rapid proliferation of high-performance and specialty polymers in the building construction, automotive, and aerospace industries. The extreme variability in chemical composition which characterizes this class of materials has created a pressing need for new and more versatile treatments for reducing flammability. The traditional "trial and error" approach does not offer an optimal solution to this problem. In the present investigation, we examine the feasibility of applying a computer model of polymer degradation and flammability to the design of fire-resistant materials.

The burning of polymeric material may be viewed as a two-step process whereby volatile fragments produced in the thermal degradation of the condensed phase mix with the ambient oxygen in the gas phase where they are combusted.<sup>1,2</sup> Much of the energy released in this process is absorbed and thermalized by the residual polymer. The cycle continues as long as there is sufficient heat to further pyrolyze the polymer into combustible products. The activity of fire retardants is due to their ability to inhibit free-radical reactions which propagate gas-phase combustion and/or to their capacity to depress the rate of evolution of volatile compounds from the condensed phase.<sup>3-5</sup>

The focus of the present investigation is on the latter effect. More specifically, we are interested in the possibility of reducing the flammability of polyethylene and related polymers by increasing their tendency to char. It is not surprising that there is a strong correlation between char residue and fire resistance,<sup>6</sup> since char is always formed at the expense of volatile fuel. Furthermore, surface char tends to insulate the unburnt material from the heat generated in gas-phase combustion.

Under normal circumstances, polyethylene does not char when it is burned. Rather, its thermal degradation is dominated by random scission of the C-C bonds followed by hydrogen transfer and disproportionation. These reactions produce a broad distribution of volatile hydrocarbons.<sup>10</sup> The fact that cross-linking predominates over scission when polyethylene is exposed to ionizing radiation,<sup>11,12</sup> however, suggests that it may be possible to alter its thermal degradation chemistry so that the formation of char is more favorable and thereby to achieve a significant reduction in flammability.

We have reported results obtained from molecular dynamic simulations of initial events in the thermal degradation of polymers in previous papers.<sup>7-9</sup> The

computer code has now been augmented to include more of the major reaction channels. In addition to random scission and depolymerization reactions, the present model also accounts for hydrogen transfer, chain stripping, radical recombination, cyclization, and intermolecular cross-linking. In this investigation, the computer model is used to identify factors which promote intermolecular cross-linking and eventually lead to the formation of high molecular weight, thermally stable chars.

## Description of the Model

**A. Molecular Dynamics.** Molecular dynamics consists of solving Hamilton's equations of motion

$$\frac{\partial H}{\partial p_i} = \frac{dq_i}{dt} \quad \frac{\partial H}{\partial q_i} = -\frac{dp_i}{dt} \quad (i = 1, 2, \dots, 3N) \quad (1)$$

for each of the  $3N$  molecular degrees of freedom. In this equation  $p_i$  and  $q_i$  denote the Cartesian components of momentum and position, respectively. The Hamiltonian of the model polymers considered in the present investigation has the form

$$H = \sum_{i=1}^{3N} \frac{p_i^2}{2m_i} + \sum_{i=1}^{N-1} V_b(r_{i,i+1}) + \sum_{i=1}^{N_C-2} V_a(\theta_{i,i+1,i+2}) + \sum_{i=1}^{N_C-3} V_t(\phi_{i,i+1,i+2,i+3}) + \sum_{i=1}^{N_C-3} \sum_{j=i+3}^{N_C} V_{nb}(r_{ij}) + \sum_{i=1}^{N_C} \sum_{j=1}^{N_s} V_{nb}(r_{ij}) \quad (2)$$

where  $N_C$  denotes the number of carbon atoms and  $N_H$  the number of hydrogen atoms. The first term on the right-hand side of eq 2 represents the kinetic energy of the  $N = N_C + N_H$  atoms in the model polymers. The next terms are the potential energies for stretching ( $V_b$ ) and bending ( $V_a$ ) the covalent bonds and a torsional potential ( $V_t$ ) which restricts rotations around the C-C bonds. These are followed by nonbonded potential energy ( $V_{nb}$ ) interactions between the atoms in the model polymers and themselves, as well as their interactions with additional  $N_s$  atoms constituting neighboring shells in the polyethylene crystal or an external surface.

The potential energy involved in stretching the C-C and C-H bonds is described by the function

$$V_b = S(r-r_d) D\{[1 - \exp(-\alpha_e(r-r_e))]^2 - 1\} \quad (3)$$

where  $r$  is the distance between covalently bonded atoms. The dissociation energy ( $D$ ), equilibrium length ( $r_e$ ), and force constant ( $k_b = 2D\alpha_e^2$ ) for the C-C bonds were

Table I  
Hamiltonian Parameters for Model Polymers

	$V_b$	$V_a$	$V_t$	$V_{nb}$	
C-C	$C = 347.6$ kJ/mol $\alpha_e = 19.24$ nm <sup>-1</sup> $r_e = 0.1529$ nm	$k_\theta = 130.0$ kJ/mol $\theta_0 = 113.3^\circ$	$\alpha = -18.41$ kJ/mol $\beta = 26.78$ kJ/mol	internal	$\epsilon = 0.4987$ kJ/mol $r^* = 0.2645$ nm
C-H	$D = 405.8$ $\alpha_e = 18.88$ nm <sup>-1</sup> $r_e = 0.1100$ nm			external	$\epsilon^a = 2.494$ kJ/mol $r^* = 0.2645$ nm
H-H	$D = 435.0$ kJ/mol $\alpha_e = 19.93$ nm <sup>-1</sup> $r_e = 0.0742$ nm				

<sup>a</sup> This is the value used in the simulation that produced the incipient char depicted in Figure 6. In all other simulations, the same values were used for both external and internal nonbonded potentials.

obtained from a least-squares fit to the harmonic potential used by Weber<sup>13,14</sup> and are listed in Table I. Values for the corresponding quantities for the C-H bonds, as well as for the H-H bonds which are needed to describe reaction channels which produce H<sub>2</sub> (eqs 12 and 14), were obtained from standard tabulations.<sup>15</sup>

The three-body bending potential energy term in eq 2 is represented by

$$V_a = S(r_{i,i+1}-r_d) S(r_{i+1,i+2}-r_d) \frac{k_\theta}{2} (\cos \theta - \cos \theta_0)^2 \quad (4)$$

where  $\theta$  denotes the angle defined by the dot product of the normalized bond vectors between three adjacent carbon atoms. The potential energy involved in deforming the  $\theta_{HCH}$  and  $\theta_{HCC}$  angles was ignored in the interest of computational efficiency. Numerical values for the force constant ( $k_\theta$ ) and the equilibrium bond angle ( $\theta_0$ ) which were used in our calculations are also reported in Table I.

Rotations about covalent bonds are restricted by a torsional potential

$$V_t = S(r_{i,i+1}-r_d) S(r_{i+1,i+2}-r_d) S(r_{i+2,i+3}-r_d) (\alpha \cos \phi + \beta \cos^3 \phi) \quad (5)$$

where the dihedral angle,  $\phi = \phi_{CCCC}$ , is defined by the three bond vectors between four adjacent carbon atoms. At the level of approximation adopted in this investigation, we do not use independent potential energy functions for the other dihedral angles,  $\phi_{HCCC}$  and  $\phi_{HCH}$ , which together with  $\phi_{CCCC}$  define the conformation about the C-C bonds. Rather, any movement in  $\phi$  is considered to produce a concomitant change in the other angles. The values of the parameters,  $\alpha$  and  $\beta$ , which are listed in Table I, were taken from ref 16.

The switching function<sup>17</sup>

$$S(r-r_d) = \frac{1}{2}(1 - \tanh(a(r-r_d))) \quad (6)$$

where  $a = 75.6$  nm<sup>-1</sup> is used to ensure that the potential energy terms in eqs 4 and 5 fall smoothly to zero as the relevant bond lengths approach the dissociation distance,  $r_d$  (0.42 nm). Admittedly, this function does not provide an optimal description of the coupling between bond bending and stretching. Indeed, molecular dynamic simulations have revealed that the rates of the unimolecular decomposition of HOOH through certain reaction channels are particularly sensitive to the parametrization used to describe this coupling.<sup>18</sup> Nevertheless, the function represented by eq 6 does have the desired qualitative behavior and should be adequate for the purposes of the present investigation. The same function is also used in our program to switch from one Morse potential to another as free-radical sites react to form new bonds. The

algorithm used to accomplish this will be described in the following section.

The nonbonded potential energy interactions are represented by the function

$$V_{nb} = 2\epsilon \left[ \left( \frac{r^*}{r} \right)^9 - \frac{3}{2} \left( \frac{r^*}{r} \right)^6 \right] \quad (7)$$

where  $r$  denotes the distance between CH<sub>2</sub> groups. In principle, the motions of all the nonbonded atoms should be coupled through eq 7. However, explicit interactions involving the hydrogen atoms were ignored in an effort to minimize the amount of computer time required for each simulation. In addition to the internal forces between the atoms which make up the polymer chains, nonbonded interactions with  $N_e = 1300$  external atoms constituting a rigid surface or neighboring chains in the polyethylene crystal were also considered. The values of  $r^*$  and  $\epsilon$  define the position of the minimum and the depth of the potential well, respectively. In some simulations, larger values of  $\epsilon$  were used for the external potential to account for the possibility that the interactions with an additive or filler might be considerably stronger than the internal forces between the polymer chains. The values used for both internal and external potentials are listed in Table I.

The equations of motion were integrated using the differential equation solver ODE.<sup>19</sup> This routine is based on a predictor-corrector algorithm and uses a variable step size. All forces were evaluated analytically from the first derivatives of eqs 3-7. The dynamic model consists of a central polymer chain surrounded by six additional chains<sup>16,20</sup> in accordance with the experimentally determined crystal structure of polyethylene.<sup>21</sup> Each chain is made up of 50 carbon atoms and 100 hydrogen atoms. This model is depicted in Figure 1 interacting with an external surface and in Figure 2 interacting with 12 neighboring chains in the polyethylene crystal.

**B. Reaction Channels.** The chains were in a planar zigzag conformation at the onset of the simulations. Thermal motion was initiated by giving each atom a three-dimensional velocity chosen at random from a uniform distribution. Once the atoms in the model polymers were set in motion, they adopted a Maxwell-Boltzmann velocity distribution.<sup>7</sup> The simulations were carried out for 5 ps at temperatures ranging from about 500 K, which is typical of the pyrolysis of polyethylene, all the way up to almost 5000 K, which was needed to degrade the polymer chains in a rigid crystal lattice within the allotted time. Reactive sites were created at random positions throughout the polymer chains as a result of bond dissociations. Typically, these sites developed a few tenths of a picosecond into the simulations. The C-C bonds, which are significantly weaker, had a tendency to break sooner and with greater frequency than the C-H bonds. The purpose of performing

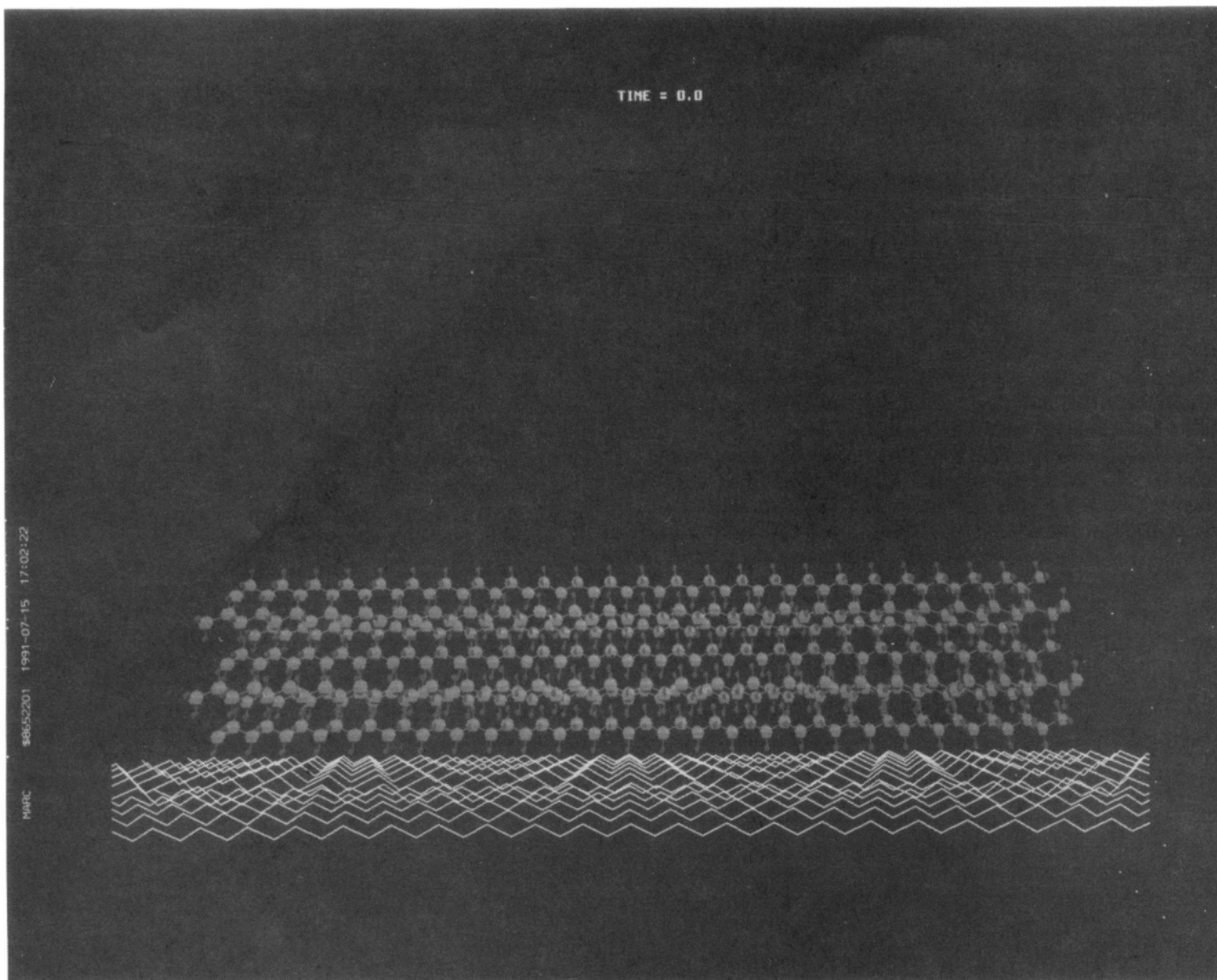
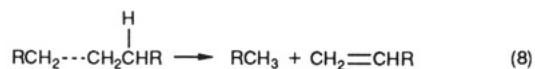


**Figure 1.** Dynamic model consisting of 7 polymer chains interacting with a rigid surface. There are 50 carbon atoms (large spheres) and 100 hydrogen atoms (small spheres) in each of the planar zigzag chains.

the high-temperature simulations was to gain insight into the differences between the thermal and radiation-induced degradation of polyethylene. Although 5000 K is unrealistically high for thermal degradation, it is not an unreasonable value for the local temperature of polymers exposed to ionizing radiation.

Two reactions which involve dissociation of the C-C bonds, and which are thought to play a major role in the thermal degradation of polymers, are hydrogen transfer and depolymerization. An example of an intramolecular hydrogen transfer reaction is depicted in the following scheme:



The resulting fragments can react again and again in recursive fashion producing a broad spectrum of volatile hydrocarbons which are readily combusted. The possibility of intermolecular hydrogen transfer between free-radical fragments is also accounted for in the computer program.

In the depolymerization reaction illustrated in eq 9 the



monomer splits off from a free-radical fragment generated

by the random scission of a C-C bond. Since ethylene comprises only a small fraction of the total hydrocarbons produced, it is presumed that the rate of hydrogen transfer is much faster than the rate of depolymerization in the low-temperature thermal degradation of polyethylene. This is not universally true. The relative rates of these reactions depend on the nature of the intramolecular forces.<sup>9</sup> Thus, polytetrafluoroethylene, for example, thermally degrades almost exclusively into monomer.<sup>10</sup>

In our computer program both hydrogen transfer and depolymerization reactions are modeled as concerted processes so that bond making occurs simultaneously with bond breaking. This is accomplished using the switching functions defined in eq 6. In the case of the depolymerization reaction, a new  $\pi$  bond forms at the same time as the adjacent  $\sigma$  bonds break. The potential energy of the  $\pi$  bond is

$$V = (1 - S(r_{ij}-r_d))(1 - S(r_{kl}-r_d))D'\{[1 - \exp(-\alpha_e(r_{j,k}-r_e))]^2 - 1\} \quad (10)$$

with  $\{i, j, k, l\}$  denoting adjacent carbons and  $D' = 0.759D_{\text{C-C}}$ , the dissociation energy of a C-C  $\pi$  bond. The net activation energy after the first random scission is, therefore, about 84 kJ/mol, which is the difference between the  $\sigma$  and  $\pi$  bond energies. A similar analysis gives the same activation energy for the reaction depicted in eq 9.

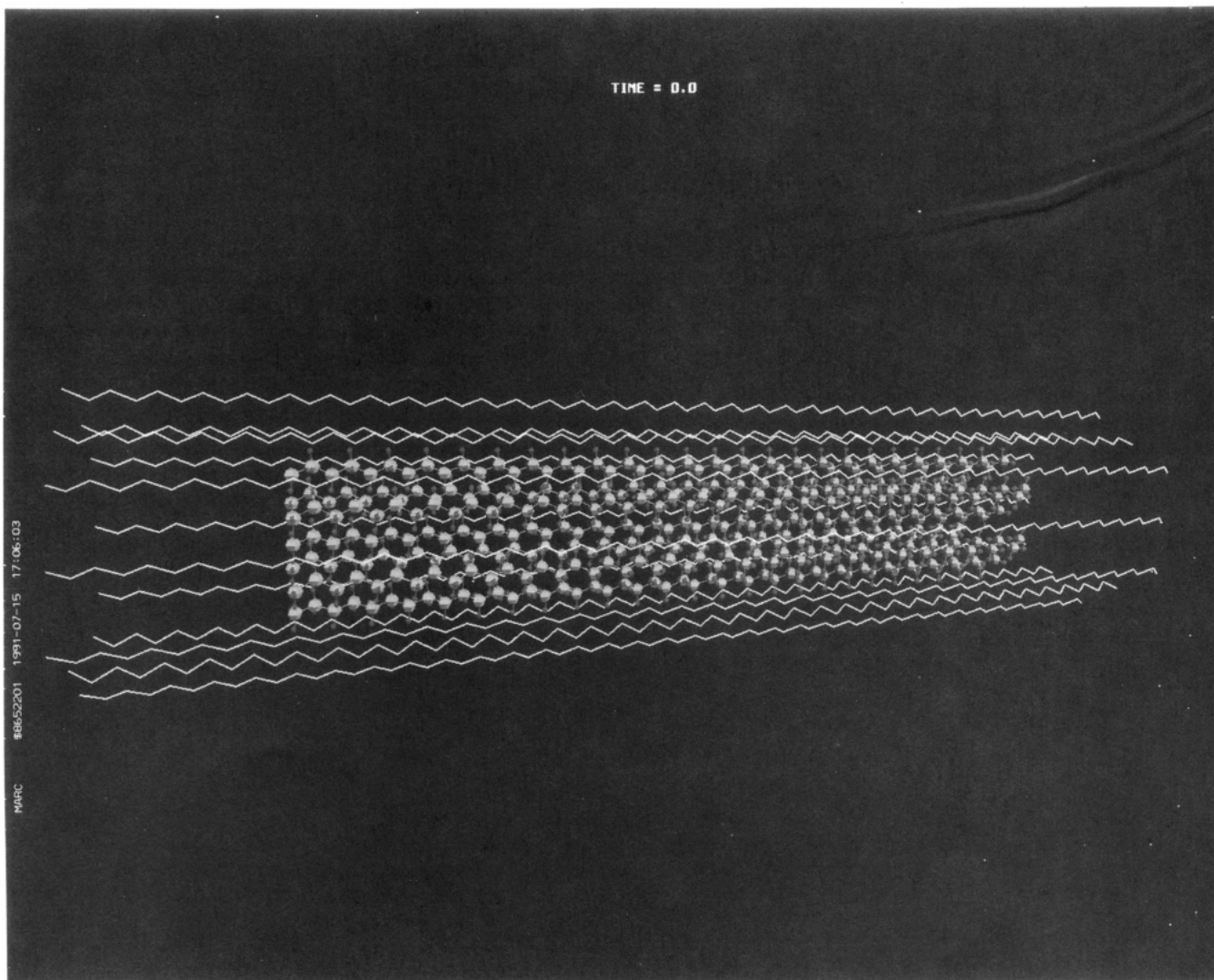


**Figure 2.** Dynamic model consisting of 7 polymer chains interacting with an additional 12 chains comprising the next-nearest-neighbor shell in the polyethylene crystal. There are 50 carbon atoms (large spheres) and 100 hydrogen atoms (small spheres) in each of the planar zigzag chains.

Presumably, hydrogen transfer dominates the low-temperature thermal degradation of polyethylene because it occurs even when there is insufficient energy to generate the free-radical fragments required for depolymerization. The activation energy for the random scission reactions which produce these fragments is approximately equal to the dissociation energy of a  $\sigma$  bond between two carbon atoms (347 kJ/mol).

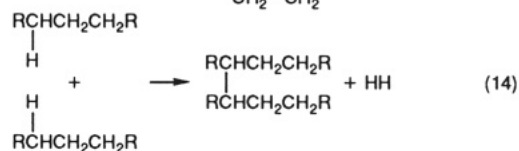
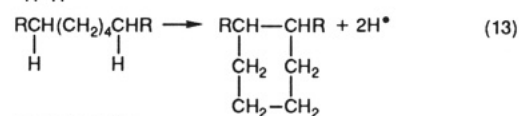
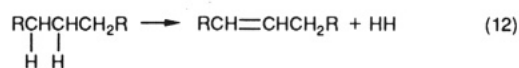
The degradation process terminates when reactive fragments combine to form more stable products. One such mechanism, which is also accounted for in the computer model, is the radical recombination reaction illustrated in eq 11.



We also allow for a number of other reaction channels which are normally inactive in the thermal degradation of polyethylene. Radical sites are generated whenever a bond begins to break. These in turn are eligible to react with other radical sites to form new bonds. This is simulated in the computer program by the following algorithm: When the length of any bond exceeds the value  $r_d - r_e$ , an attempt is made to form a new bond by examining all possible covalent interactions. The potential energy is given by eq 10, where  $D'$  is the dissociation energy of the new bond

that forms between atoms  $j$  and  $k$  when the  $i-j$  and  $k-l$  bonds break. The trajectories are updated only on the basis of the forces corresponding to the minimum energy subject to the constraints that there are never more than four bonds to a carbon and more than one bond to a hydrogen atom.

In addition to the vinylic compounds and monomers which are produced in the reactions outlined in eqs 8 and 9, vinylenic, cyclic, and cross-linked hydrocarbons are also formed. Examples of the chain stripping, cyclization, and intermolecular cross-linking reactions which give rise to these products are illustrated in eqs 12–14. These reactions differ from hydrogen transfer and depolymerization in



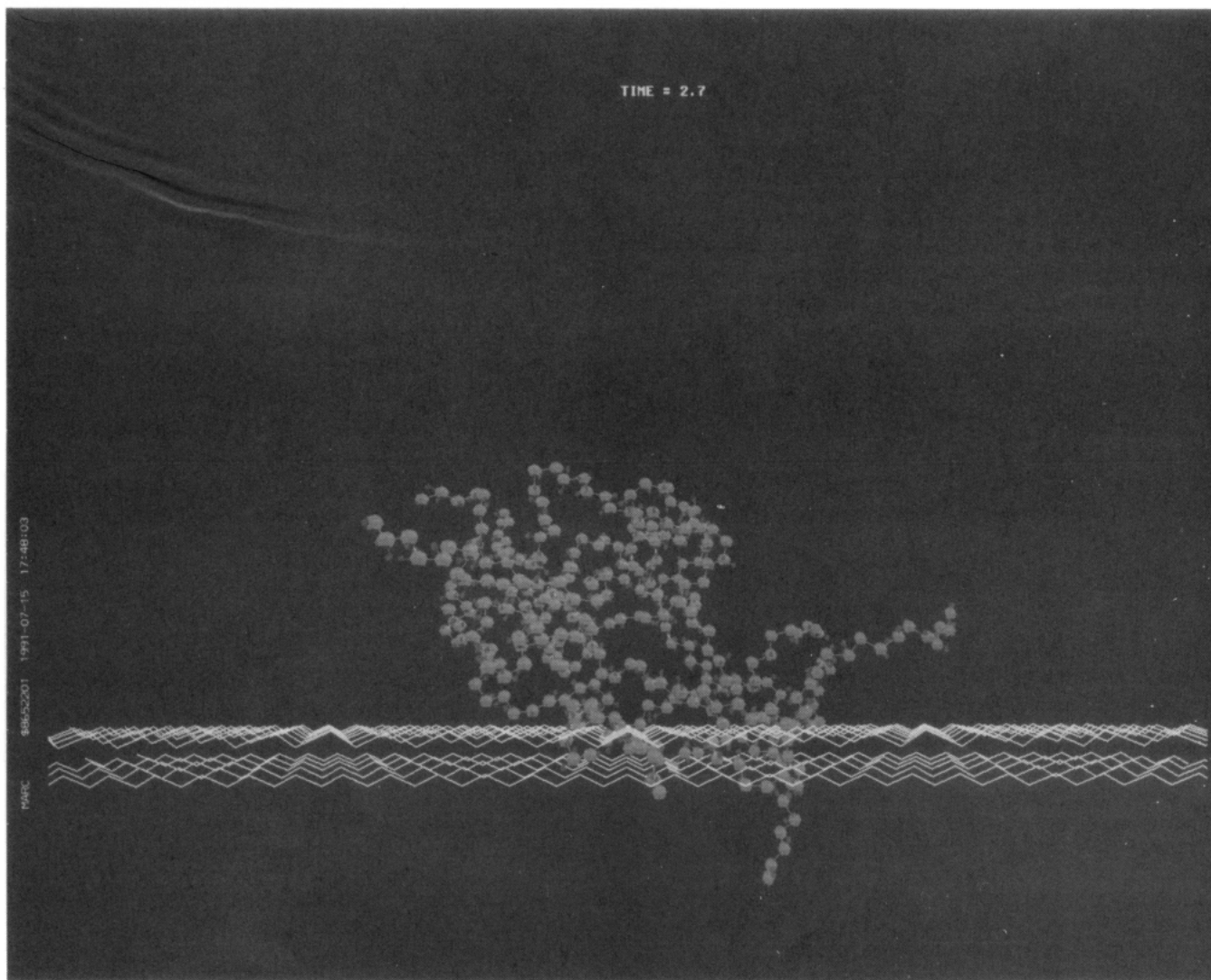


**Figure 3.** Polymer chains coiled into a ball-like structure during the early stages of the thermal degradation of polyethylene.

that they involve the formation rather than the dissociation of C–C bonds. The new bonds result from the lowest energy interactions between the radical sites created by random scission of the C–H bonds. Thus, it is the distance between the radical sites which determines which of these reactions will occur. If the distance between radical sites is greater than  $r_d$ , as would be expected for the H atoms in the reaction depicted in eq 13, then they will not form a bond.

## Results and Discussion

**A. Computer Simulations.** The scene depicted in Figure 3 is representative of the prevailing conditions during the early stages of the thermal degradation of polyethylene. The polymer chains, which are too big to move away from each other as long as they remain intact, are coiled into a ball-like structure which brings nascent radical sites from neighboring chains into close proximity. Although this arrangement would be favorable for the formation of cross-links, it is destroyed before a significant number of radical sites can develop as the mobile fragments produced in random scission of the C–C bonds volatilize as fuel (Figure 4). It is clear that intermolecular cross-linking cannot be a significant degradative pathway in polyethylene as long as the backbone fragments before the C–H bonds break.

This is not always the case. Despite the fact that the C–C bonds are significantly weaker than the C–H bonds,

cross-linking predominates over scission when polyethylene is exposed to ionizing radiation. A major factor which contributes to this effect is that the structure of the solid is retained when the polymer is irradiated. The lattice forces restrict the movement of free-radical fragments so that they remain trapped until they combine with other radicals in accordance with the reaction scheme summarized in eq 11. On the other hand, the hydrogen produced in reactions of the type illustrated in eq 14 can readily escape. A related phenomenon, sometimes referred to as the "cage effect", does influence the thermal degradation of polymer chains in the interior of a solid. The consequences, however, are less pronounced than they are in radiation-induced degradation because of the increase in polymer mobility which is the inevitable precursor to thermal degradation.

While the forces in the solid tend to promote intermolecular cross-linking, they also prevent the radical sites from getting close enough to make strong covalent bonds. This has an adverse effect on the stability of the cross-linked structures that are formed so that room-temperature irradiation tends to produce a network consisting of elongated and highly strained cross-links. This explanation is consistent with the experimental observation that the efficiency of radiation cross-linking in polyethylene increases with increasing temperature (and hence the mobility of the chains) between 50 and 250 °C.<sup>11</sup> These effects are evident in Figure 5 which depicts the degra-

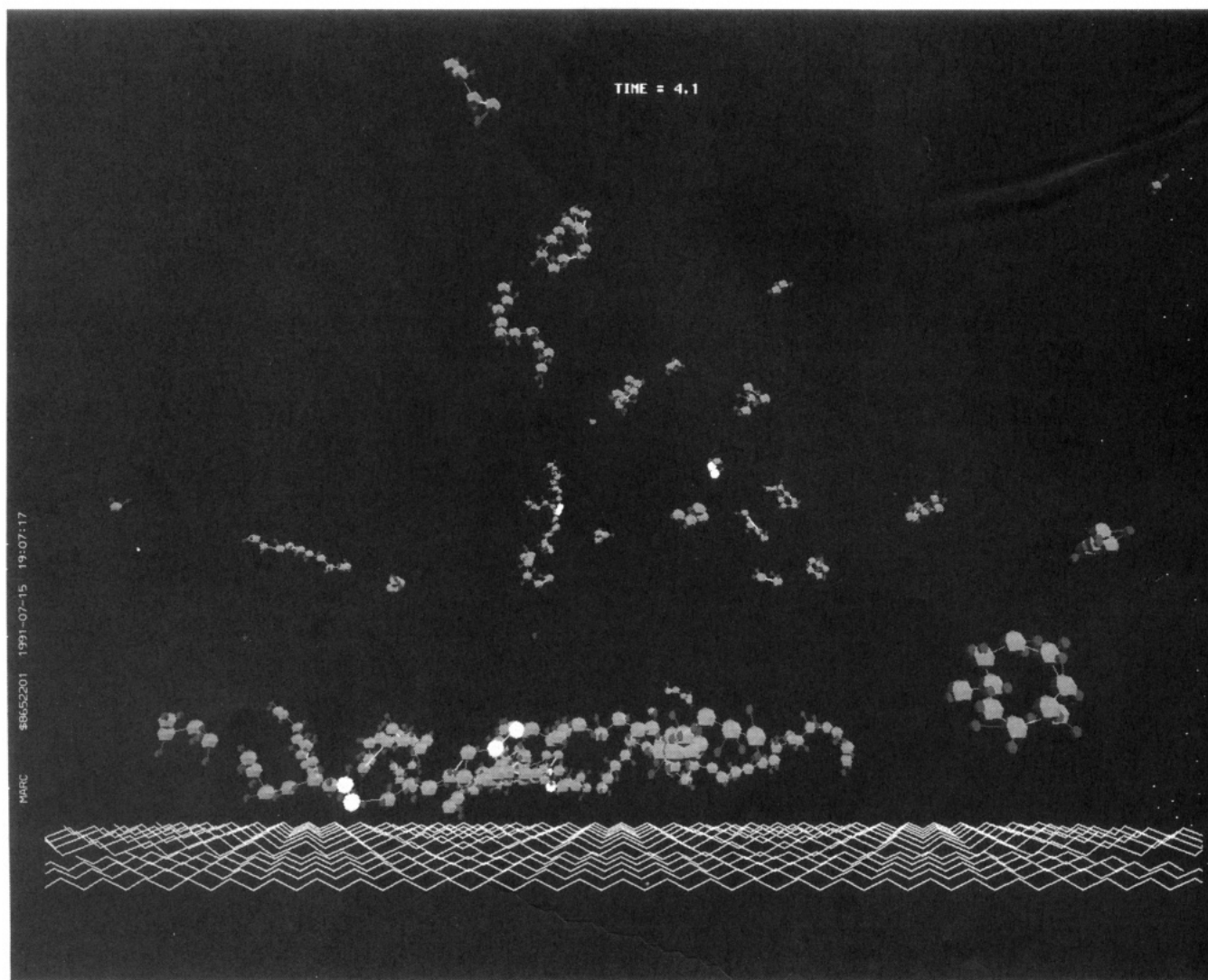


**Figure 4.** Mobile fragments which are produced by random scission of the C-C bonds volatilizing as fuel for gas-phase combustion reactions. The temperature at this point in the simulation (4.1 ps) is approximately 1500 K.

dation of polyethylene chains in a crystal.

During the initial stages of thermal degradation the structure of the solid begins to break down. Computer movies of the trajectories obtained from molecular dynamic simulations indicate that the polymer network, which contains many elongated and highly strained intermolecular bonds at room temperature, responds by forming stronger cross-links. The presence of these cross-links makes fragmentation of the backbone during thermal degradation more difficult. At some point, the rate of C-H bond dissociations will exceed the rate at which mobile fragments are produced and a char should form. This hypothesis was examined by performing the computer simulations of thermal degradation after removing hydrogens from random sites in the model polymers.

Our model of thermal degradation may be viewed as a kinetic competition between random scission, depolymerization, hydrogen transfer, radical recombination, chain stripping, cyclization, and cross-linking. A char results when the prevailing conditions favor the formation of intermolecular cross-links over the other reaction channels. This balance is precarious because the temperature, and therefore the rate of thermal degradation, increases dramatically as new bonds are formed in the incipient char. Both the number of initial radical sites and the nature of the nonbonded interactions exert a strong influence on the kinetic competition between these re-

actions. Thus, we found that those model polymers which had fewer than  $\approx 100$  hydrogens removed tended to fragment and depolymerize rather than char. Likewise, char did not form for values of  $r^*$  greater than  $\approx 0.3$  nm because the carbon atoms could not get close enough to form stable cross-links. We also discovered that the extent of intermolecular cross-linking increased with the magnitude of the surface forces. Presumably, this is because the polymer chains are brought closer together as a result of their mutual attraction to the surface. In the simulation that produced the incipient char depicted in Figure 6,  $\epsilon_s$  was 2.5 kJ/mol, 5 times the value used in the other simulations. This observation suggests that the presence of a filler, particularly one that has a strong affinity for the polymer, will facilitate the formation of char.

**B. Experimental Validation.** Standard reference polyethylene (SRM 1496)<sup>22</sup> having a density of 0.93 g/cm<sup>3</sup> and a weight-average molecular weight ( $M_w$ ) of 170 000 was used in these experiments. Samples were  $\gamma$ -ray-irradiated in a Nordion gammacell 220 (<sup>60</sup>Co source) at room temperature in a vacuum. [Certain commercial equipment, instruments, or materials are identified in this paper in order to adequately specify the experimental procedure. Such identification does not imply that the material or equipment identified is necessarily the best available for the purpose.] They received a dose of 100 Mrad at an average rate of 0.7 Mrad/h. This works out

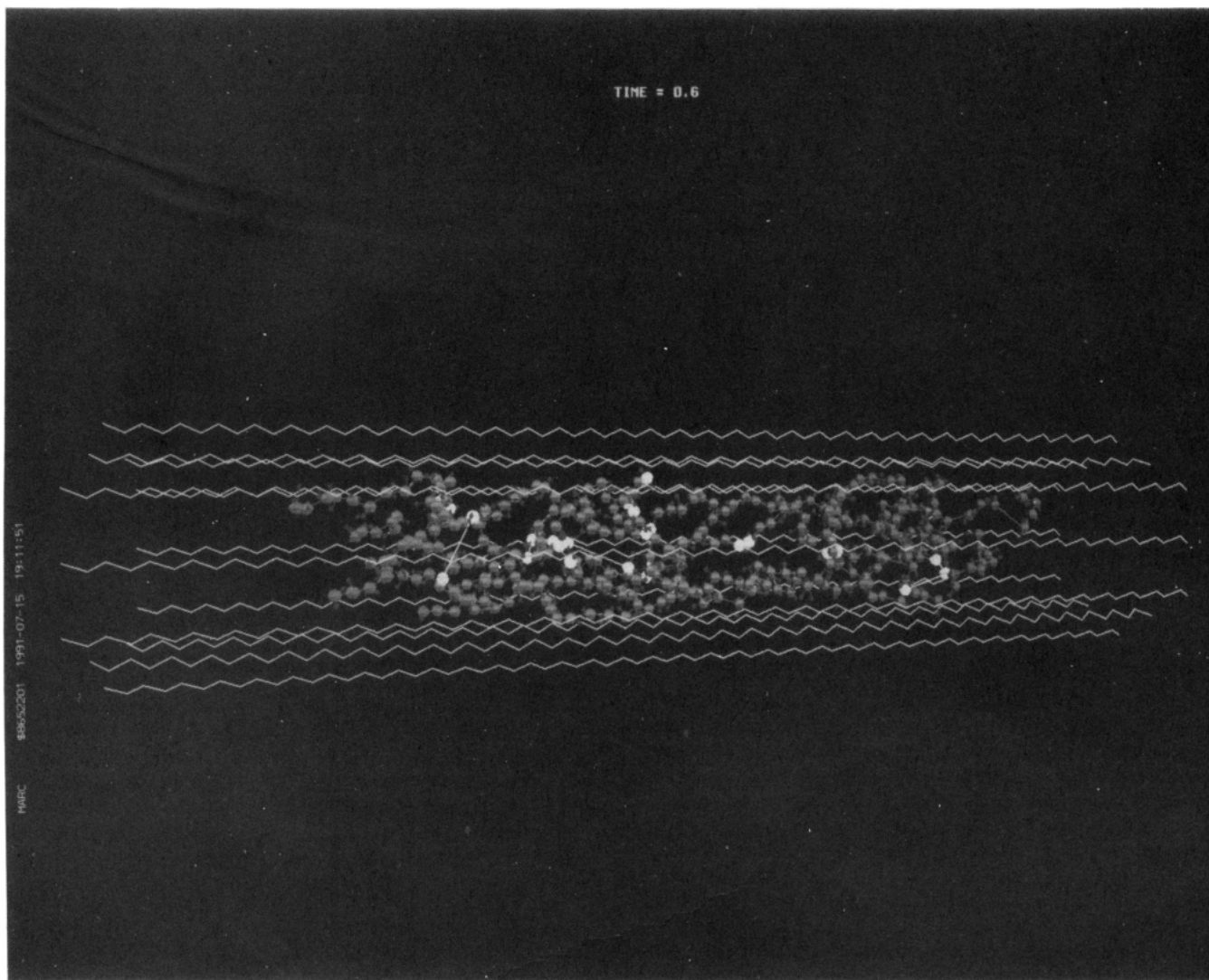


**Figure 5.** High-temperature ( $\approx 5000$  K) thermal degradation of polyethylene in a rigid lattice producing highly strained intermolecular cross-links (highlighted by large white spheres) from the radical sites created by random scission of the C-H bonds. Several of these free hydrogens (small spheres) appear to have migrated away from the lattice.

to an average of about 140 hydrogen atoms lost per polymer chain based on  $G(\text{H}_2) = 4$  (i.e., 4 hydrogen molecules formed for every 100 eV of energy absorbed by the sample), which is representative of the values reported in the literature.<sup>11,12</sup> No attempt was made to exclude oxygen after removing the samples from the gammacell. The material was observed to yellow over a period of several weeks. This progression, from a mild tint to an obvious yellow, was presumably due to reactions involving trapped radicals. The discoloration was still faint when the thermogravimetric (TG) and flammability measurements were performed about 72 h after the irradiation.

A Mettler TA12 was used in the thermogravimetric analyses of the linear and  $\gamma$ -ray-irradiated polyethylene samples. The analyses were performed in air with a heating rate of  $5^\circ\text{C}/\text{min}$  up to a final temperature of  $580^\circ\text{C}$ . The derivative thermograms displayed in Figure 7 indicate that the  $\gamma$ -ray-irradiated sample is more thermally stable since its decomposition is shifted toward higher temperatures by about  $20^\circ\text{C}$ .

Ignition and flammability tests were made with the NIST Cone Calorimeter. This instrument measures a number of combustion-related properties including the rate of heat release from oxygen consumption and is the basis for the ASTM test method E1354-90a.<sup>23</sup> Both samples were placed in a glass dish and exposed to a radiant

energy flux of  $20\text{ kW}/\text{m}^2$ . A high voltage arc was placed above the samples to ignite the off-gases. The time to ignition for the linear polyethylene was about 285 s. Once ignited, it almost completely volatilized, leaving only a very thin coat of soot on the walls of the glass container. The  $\gamma$ -ray-irradiated polyethylene, however, ignited only after 925 s had elapsed. The irradiated sample then underwent flaming combustion which consumed approximately 95% of its original mass. After an additional 900 s, the sample self-extinguished, leaving behind a brittle char. The delay in time to ignition and the presence of a residual char confirm that the  $\gamma$ -ray-irradiation was effective in reducing the flammability of polyethylene.

## Conclusions

Molecular dynamics can provide a realistic description of the thermal degradation of polymers and should, therefore, aid in the development of fire-retardant treatments for these materials. In the present investigation, we demonstrated this utility by using this technique to identify factors which might be effective in reducing the flammability of polyethylene by promoting the formation of a residual char. Computer movies of the calculated trajectories indicated that a significant reduction in the flammability of polyethylene could be achieved through radiation cross-linking. This prediction was confirmed in

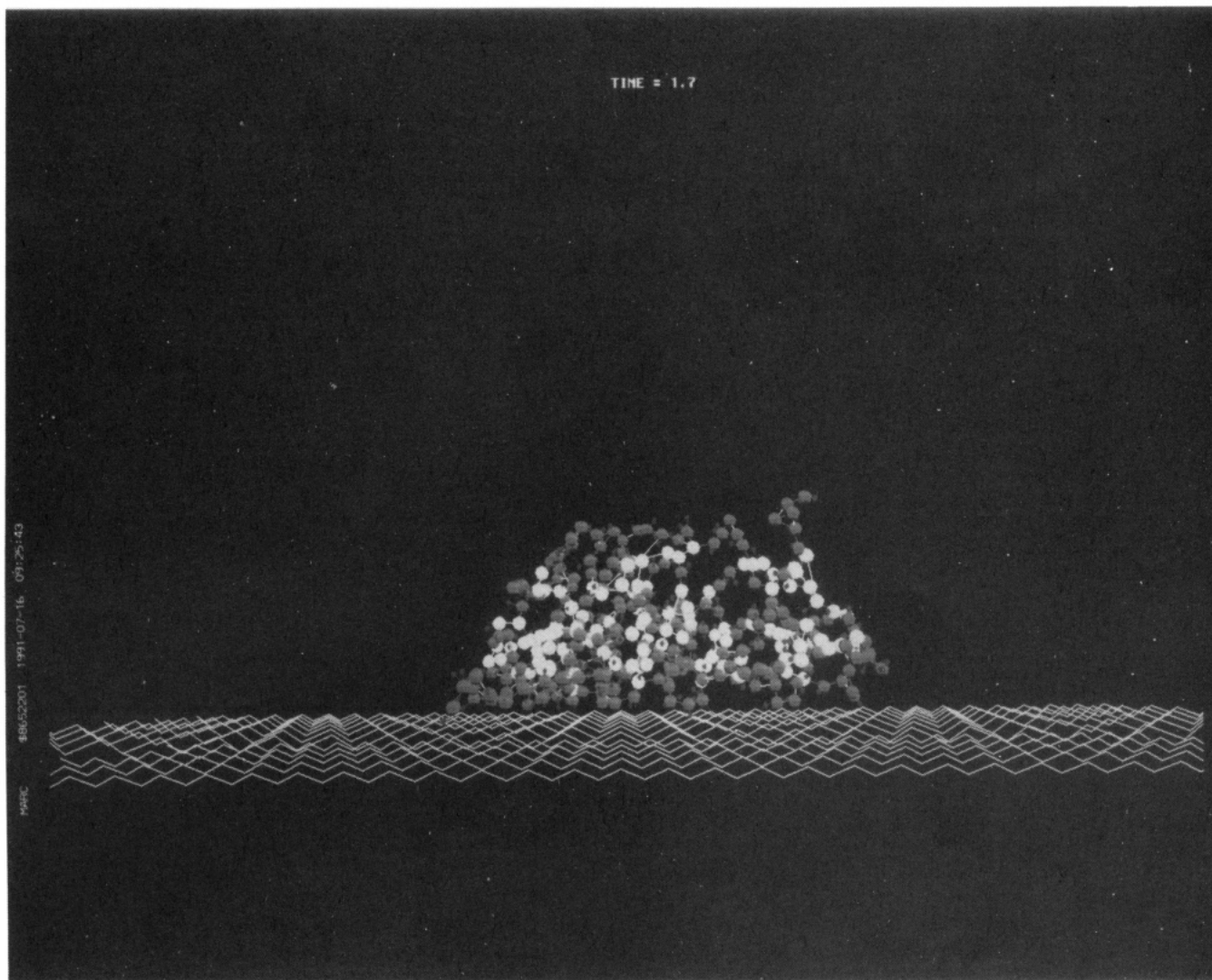


**Figure 6.** Incipient char, which is indicated by the high density of white spheres, formed when there are a large number of radical sites in close proximity. In this simulation, which was initiated at 500 K, the polymer chains were brought close together by their mutual attraction to the rigid surface. A total of 350 hydrogens were removed from the model polymers prior to the initiation of the thermal motion.

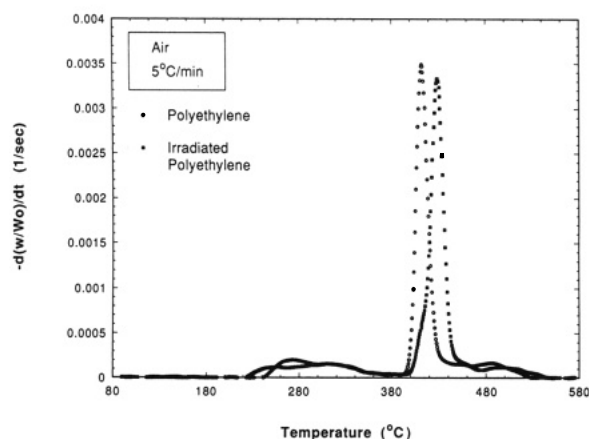


**Figure 7.** Comparison of the derivative thermograms obtained from samples of linear (denoted by open circles) and  $\gamma$ -ray-irradiated polyethylene (denoted by filled squares).

TG and flammability measurements of linear and  $\gamma$ -ray-irradiated polyethylene.

Future research will involve performing additional simulations to determine conditions which maximize fire resistance while minimizing treatment costs and the loss of intended-use properties. Efforts will also be directed

at finding chemical cross-linking agents which are inert at ambient temperatures but activate at the onset of thermal degradation.

**Acknowledgment.** We are grateful to Dr. James Humphreys of NIST for performing the  $\gamma$ -ray irradiations and to Robin Breese, also of NIST, for performing the TG analyses. We also thank Dr. D. W. Noid of Oak Ridge National Laboratory and Dr. Barry Bauer of NIST for their guidance.

#### References and Notes

- (1) Cullis, C. F.; Hirschler, M. M. *The Combustion of Organic Polymers*; Clarendon Press: Oxford, 1981.
- (2) Pearce, E. M.; Khanna, Y. P.; Raucher, D. In *Thermal Characterization of Polymeric Materials*; Turi, E. A., Ed.; Academic Press: New York, 1981; pp 793-843.
- (3) Lyons, J. W. *The Chemistry and Uses of Fire Retardants*; Wiley-Interscience: New York, 1970.
- (4) Chamberlain, D. L. In *Flame Retardancy of Polymeric Materials*; Kuryla, W. C., Papa, A. J., Eds.; Marcel Dekker: New York, 1978; pp 109-168.
- (5) Shafizadeh, F.; Chin, P. S.; DeGroot, V. F. *J. Fire Flamm./Fire Retard. Chem.* **1975**, *2*, 1975.
- (6) van Krevelen, D. W. *Polymer* **1975**, *16*, 615.
- (7) Nyden, M. R.; Noid, D. W. *Phys. Chem.* **1991**, *95*, 940.
- (8) Blaisten-Barojas, E.; Nyden, M. R. *Chem. Phys. Lett.* **1990**, *171*, 499.

- (9) Nyden, M. R. *Polym. Prepr. (Am. Chem. Soc., Div. Polym. Chem.)* **1989**, *30*, 98.
- (10) Madorsky, S. L. *Thermal Degradation of Organic Polymers*; Wiley-Interscience: New York, 1964.
- (11) Chapiro, A. *Radiation Chemistry of Polymeric Systems*; Wiley-Interscience: New York, 1962.
- (12) Dole, M. In *Crystalline Olefin Polymers*; Raff, R. A. V., Doak, K. W., Eds.; Wiley-Interscience: New York, 1965; Part 2, pp 845-977.
- (13) Weber, T. A. *J. Chem. Phys.* **1978**, *69*, 2347.
- (14) Weber, T. A. *J. Chem. Phys.* **1979**, *70*, 4277.
- (15) Herzberg, G. *Spectra of Diatomic Molecules*; Van Nostrand: Princeton, NJ, 1950. Herzberg, G. *Infrared and Raman Spectra*; Van Nostrand: Princeton, NJ, 1945.
- (16) Noid, D. W.; Sumpter, B. G.; Wunderlich, B. *Macromolecules* **1990**, *23*, 664.
- (17) Arfken, G. *Mathematical Methods for Physicists*; Academic Press: London, 1970; p 419.
- (18) Getino, C.; Sumpter, B. G.; Santamaria, *Chem. Phys.* **1990**, *145*, 1.
- (19) Shampine, L. F.; Gordon, M. K. *Computer Solutions of Ordinary Differential Equations: The Initial Value Problem*; W. H. Freeman: San Francisco, 1975.
- (20) Reneker, D. H.; Mazur, J. *Polymer* **1988**, *29*, 3. Reneker, D. H.; Mazur, J. *Crystallographic Defects in Polymers and What They Do*. *Polym. Prepr. (Am. Chem. Soc., Div. Polym. Chem.)*, in press.
- (21) Bunn, C. W. *Chemical Crystallography an Introduction to Optical and X-Ray Methods*, 2nd ed.; Clarendon Press: Oxford, 1961.
- (22) Crissman, J. M.; Wang, F. W.; Guttman, C. M.; Maurey, J. R.; Wagner, H. L.; Fanconi, B. M.; VanderHart, D. L. NBSIR 87-3506; U.S. Department of Commerce, NIST: Gaithersburg, MD.
- (23) *Standard Test Method for Heat and Visible Smoke Release Rates for Materials and Products Using an Oxygen Consumption Calorimeter*; ASTM: Philadelphia, PA, 1991; pp 1-17.

**Registry No.** Polyethylene, 9002-88-4.